Advances in Nano Research, *Vol. 10, No. 6 (2021) 517-529*
DOI: https://doi.org/10.12989/anr.2021.10.6.517

The economic and management use of rhododendron petals in potas-sium-ion nano batteries anode via efficient computer simulation

Wensheng Dai*[1], Yousef Zand[2], Alireza Sadighi Agdas[3], Abdellatif Selmi[4,5], Angel Roco-Videla[6,7], Karzan Wakil[8,9] and Alibek Issakhov[10,11]

[1]*Financial School, China Financial Policy Research Center, International Monetary Institute, Renmin University of China, Beijing 100872, China*
[2]*Department of Civil Engineering,Tabriz Branch, Islamic Azad University, Tabriz, Iran*
[3]*Ghateh Gostar Novin Company, Tabriz, Iran*
[4]*Department of Civil Engineering, College of Engineering, Prince Sattam bin Abdulaziz University, Al-Kharj 11942, Saudi Arabia*
[5]*Ecole Nationale d'Ingénieurs deTunis (ENIT), Civil Engineering Laboratory, B.P. 37, Le belvédère1002, Tunis, Tunisia*
[6]*Programa Magister en ciencias químico-biológicas, Facultad de Ciencias de la Salud, Universidad Bernardo O´Higgins, Santiago-Chile*
[7]*Departamento de ingeniería Civil, Facultad de Ingeniería, Universidad Católica de la Santísima Concepción, Concepción-Chile*
[8]*Department of Computer, College of Science, University of Halabja, Halabja 46018, Kurdistan Region, Iraq*
[9]*Research Center, Sulaimani Polytechnic University, Sulaimani 46001, Kurdistan Region, Iraq*
[10]*Al-Farabi Kazakh National University, Almaty, Kazakhstan*
[11]*Kazakh-British Technical University, Almaty, Kazakhstan*

(*Received January 21, 2020, Revised February 13, 2021, Accepted February 19, 2021*)

Abstract. Nano batteries are manufactured batteries which use nanoscale technology, small particles measuring less than 100 nanometers or 10-7 meters. In addition, because of plentiful potassium supplies and less cost, potassium-ion batteries (PIBs) are taken as possible substitutes for lithium-ion batteries for massive energy storing systems. Our modern lifestyle could be totally different without rechargeable batteries. Regarding their economic and management usage, these batteries are applied in electric and hybrid vehicles, devices, and renewable power generation systems. Accordingly, regarding the huge K ion radius, it is a difficult process for identifying relevant materials with excellent cycling stability and capacity. At present, the production of suitable anode materials with high specific capacities, long cycle life and low costs for PIBs remains a major challenge. Also, the continuing improvement in defining future electors, the manufacture of PIBs has been complicated by multiple challenges, namely low reversible performance, insufficient cycling stability and poor energy density, all of which have created important doubts for the effective implications of PIBs. Nano-particles have shown various advantages for enhanced energy and power density, cyclability and safety when it comes to designing and producing electrode materials via efficient computer simulation. In combination with large volume expansion, slow reaction kinetics, and low electrical conductivity the main cause for the degradation of SnO_2 reaction reversibility and power decay observed are not as obvious as those of Lithium-ion batteries (LIBs) as anodes of sodium-ion batteries (SIBs), and potassium-ion batteries (KIBs).

Keywords: biomass; hard carbon; potassium-ion batteries; nitrogen-doped; energy storage mechanism

1. Introduction

In 2018, the global demand for energy storage was estimated at $72 billion and is projected to rise to $165 billion before 2025 (Dyatlov *et al.* 2020). The global battery market has been estimated to be progressed by 6.63% CAGR during the expected years of 2019-27 (Baumann *et al.* 2021). In addition, the energy crisis on Earth is disrupting the growth and creating difficulties for human survival (Mehtab *et al.* 2019, Yang *et al.* 2020a, Yasin *et al.* 2020). The need for physically small batteries is growing rapidly with the growth in need for portable electronics (Shi *et al.* 2020, Fujita *et al.* 2021, Zhang *et al.* 2021). Thus, the miniaturization of the battery is a critical task that the battery community must take into account. For especial purposes, namely micro-electromechanical systems and chips, nano-scale batteries are used extensively (Chen *et al.* 2018, Lei *et al.* 2020). Regarding the use of computer simulation, nano battery incorporated in device indicates that power sources are also important in the process of miniaturization. The key characteristics of Nano batteries with dimensions of 1 cm^2 (Lowy *et al.* 2008) are their energy and power densities. When these tiny devices are integrated in parallel, then thousands of Nano batteries could be placed on 0.5-mm-thick substrate which can have a charge of up to 10-mAh cm^2 power per footprint. These batteries were evaluated for a significant number of charge-discharge rounds, without compromising their stability and capacitance. In addition, this design provides a massive electrical power output that eliminates the risk of flammability, a big source of malfunctioning in laptop and mobile batteries. Novel battery technologies in nano world

*Corresponding author, Professor, Ph.D.,
E-mail: 438616074d@mail.com

ISSN: 2287-237X (Print), 2287-2388 (Online)

allow Nano battery systems to stay operational for a minimum duration of 15 years (Ni *et al.* 2019a, b, Ning *et al.* 2020). The advancement of energy storage systems by waste management focuses on advanced energy technology. The lightweight N-S doped carbon nanofibers as hybrid condensers would be promoted by it. The satisfactory electrochemical results encourage the principle of waste management in order to scalable energy storage device efficiency (Zuo *et al.* 2015, 2017, Zhang *et al.* 2020a). The Nano battery can apply both to Nano sized batteries, as well as to the use of macroscopic battery nanotechnology to improve its efficiency and lifespan (Rouhanifar *et al.* 2019, Hu *et al.* 2020, Yang *et al.* 2020b). Nano battery can deliver many benefits, including fast charging, higher power density, and prolonged shelf life over the conventional battery (Guo *et al.* 2020, Wang *et al.* 2020, Yan *et al.* 2021). For a primary (non-rechargeable) battery, it is possible to use nanotechnology to obtain a high-performance primary battery. Iost *et al*. (2016) stated using monolayer graphene to provide an initial battery on a chip. For several hours, their batteries produced a steady voltage (1.1 V) with a high 15 μAh power. Nano-MnO^2 was utilized as a cathode material (Srither *et al.* 2013) to improve the discharge power and energy density of magnesium primary batteries. Srither *et al*. (2014) published similar findings in the primary cell of Zn/MnO_2 for the improvement of discharge power retention and shelf life. In the high-power alkaline $Zn\text{-}MnO_2$ batteries (Cheng *et al.* 2005), γ-MnO_2 nanowires/ nanotubes could be used. The multi-walled carbon nanotube (MWCNT)-templated cobalt phthalocyanine (CoPc) can increase its discharge energy as a catalyst for the $Li/SOCl_2$ battery (Xu *et al.* 2010). Wei *et al*. (2017) manufactured a hybrid nanomaterial (acetylene black nanoparticles/ graphene nano sheets) as a high-discharge $Li/SOCl_2$ battery cathode material (1706 mAh/g capacity at 5 mA/cm^2 current density). Sun *et al*. (2016) developed an electrode on the basis of nano-V, Ti-doped MnO_2 for high-rate batteries for the $Li\text{-}MnO_2$ battery. For secondary (rechargeable) batteries, Douglas *et al*. (2015) have suggested that the sodium-sulfur and lithium-sulfur conversion reactions for successful batteries were improved by FeS_2 nanoparticles (4.5 nm). The author stated that while conversion reaction was occurring, the scale of the nanoparticles was close to the diffusion length of iron, hence resulting in reversible and efficient cation trades. The insertion of nano-Al_2O_3 particles into the sulfur electrode in the lithium/sulfur battery not only stopped the breakdown of lithium polysulfides into liquid electrolytes, facilitated the redox reaction of lithium/sulfur (Choi *et al.* 2007, Liu *et al.* 2021). Various nanomaterials like nano-Si (Teki *et al.* 2009, Yoo *et al.* 2013), C/Si nanocomposite (Si *et al.* 2009), grapheme (Kim *et al.* 2011a, b), nano-SnO (Li *et al.* 1999), $ZnMn_2O_4$ nanowires (Kim *et al.* 2011c), core-shell Sn@Cu nanoparticles (Kim *et al.* 2010), nano-$TiNb_2O_7$ (Tang *et al.* 2013), antimony hollow Nano spheres (Hou *et al.* 2014), nano-Sb (He *et al.* 2014), nano-$ZnFe_2O_4$ (Xing *et al.* 2012), MoO_3/conducting polymer nanocomposite (Liu *et al.* 2014, Habibi *et al.* 2019a), and nano-Al (Sharma *et al.* 2013) have been used regarding to nanostructured anodes in rechargeable batteries. In addition to the experimental studies and numerical analysis, Artificial intelligence (AI) as one of the accurate, fast and cost-effective techniques have been deployed extensively in different applications (Safa *et al.* 2020, Shariati *et al.* 2020d, Yazdani *et al.* 2020). Machine learning (ML) can be used as a subset of AI to optimize and predict the performance of battery systems (Mohammadhassani *et al.* 2013, Safa *et al.* 2016, Toghroli *et al.* 2016, Mansouri *et al.* 2019). ML also can provide self-learning from data and then without human interference apply that learning. In fact, big data techniques and ML methods have addressed the different problems of modelling the relationship between complex physical characteristics and material properties (Mohammadhassani *et al.* 2014b, Chahnasir *et al.* 2018, Sedghi *et al.* 2018, Katebi *et al.* 2019). Moreover, with the ongoing progress of theories and methods, the subjects in which ML can be employed will be more widespread and have a growing influence on the effectiveness of the investigations (Shariati *et al.* 2019d, e, Trung *et al.* 2019a, Huang *et al.* 2021). Clean and green technology, for example solar, wind, tide, and geothermal has a significant role in recognizing the improvement of human society because of the reduction of environmental destruction, and fossil fuels, thereby becoming the fastest-growing renewable energy alternatives (Shariati 2020, Shariati *et al.* 2020c, f, Rajaei *et al.* 2021). These renewable energies, though, are also essentially intermittent, leading in a tension between the time and space dimensions of energy harvesting and consumption (Naghipour *et al.* 2020a, Shariati *et al.* 2020a, g). To this end, an efficient resolution for storing and distributing these transient energies is known to be the Energy Storage System (ESS) (Shariati 2008, Safa *et al.* 2019, Naghipour *et al.* 2020b, Shariati *et al.* 2020b). LIBs are the prevalent ESS technology at present and, due to their ease, high energy densities and shortage of memory feature have become important in our lives (Shariati *et al.* 2019a, 2020e, Afshar *et al.* 2020). With a gradual increment in LIB uses, due to the relative shortage (0.0017 wt percent in the Earth's crust) and inconsistent lithium source allocation, LIBs could rarely fulfill the growing demand for the future ESS (Chen *et al.* 2019, Shariati *et al.* 2019c, Trung *et al.* 2019b). As a probable alternative to LIBs, due to their low cost, and high sodium availability in the Earth's crust, SIBs have acquired a lot of interest. However, Na/Na+'s comparatively high-standard redox potential (-2.71V vs. the standard hydrogen electrode) [SHE] contributes to the lower energy density of SIBs than that of LIBs, allowing their use in portable electronics and electric cars. Compared to KIBs and SIBs, LIBs have three major potassium advantages. One of these advantages is K/K+'s smaller standard redox potential (-2.93V vs SHE), being much similar to that of Li/Li+(-3.04V vs SHE). This feature allows KIBs to have an energy density that is potentially higher than SIBs. Another advantage is having a lower cost of KIBs because of the high amount of potassium in the Earth's crust. Lastly, the weaker Lewis acidity and the corresponding lower K+ radius of Stokes than those of both Li+ and Na+ can result in the electrolyte's maximum conductivity and ion mobility of K+. It should, however, be acknowledged that four major issues are still present in the latest developments of KIBs.

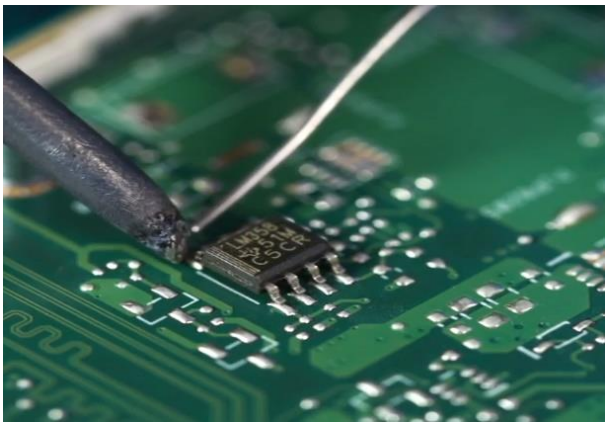

Fig. 1 Micro batteries

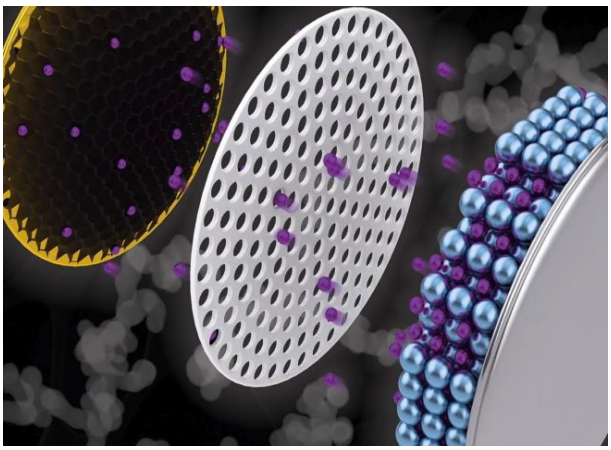

Fig. 2 The structure of batteries

First of all, there is still a shortage of KIB electrodes with high ability to ensure high energy density. Secondly, the rate of function of KIBs is constrained by the comparably low diffusivity in solid electrodes of strong K+ ions. Thirdly, since the solvent in the electrolyte is more readily decreased on the surface of electrode, the low electrochemical capacity of K+/K leads to more side reactions. Ultimately, the electrode materials of KIBs typically are affected by pulverization-induced power fading, leading from a large volume expansion along the phase of potassiat ion/ de potassiat ion which are often plagued by large K+ ions. Several research efforts are concerned with figuring out the electrochemical method to effectively address of these issues and to significantly increase the efficiency of KIB energy storage to meet these obstacles (Chernogorov *et al.* 2017, Cao *et al.* 2020b, Chen *et al.* 2020, Liu *et al.* 2020). The production of low-cost and high-performance battery structures are needed in order to meet the increasing requirements for power sources in electric vehicles, handheld devices, and massive energy storage cases (Zhang *et al.* 2020b, c, Kang *et al.* 2021). At the present time, the market is predominantly controlled by lithium-ion batteries (LIBs); but the sustainable usage of LIBs, given the shortage and increasing prices of lithium resources, raises major concerns for the near future (Shariati 2013, Suhatril *et al.* 2019, Toghroli *et al.* 2020).

A search for possible options as substitutes for LIBs has been motivated due to the mentioned concerns. Hence, recently, batteries based on earth-rich components have gained a lot of attention, namely Mg-ion batteries, Na-ion batteries (NIBs),= and Al-ion batteries. Additionally, Potassium has desired characteristics in usage of battery, including high voltage and decent rate capability, which is found in abundance and is a low-cost element. Some attempts were done for creating KIBs. Latest KIB researches were primarily focused on the creation of carbon-based anodes, comprising graphite, carbon nanofiber, hard carbon, and graphene (Yu *et al.* 2020, Zuo *et al.* 2020, Lei *et al.* 2021). Whilst, the broad potassium ion radius (1.38 Å) makes it challenging for potassium ions to be introduced into intercalation-type electrodes, thus limiting the usage of these anodes to KIBs. The alloying mechanism, driven by information of LIBs, may be a possible way of solving this topic (Toghroli *et al.* 2017, Milovancevic *et al.* 2019, Sajedi *et al.* 2019). Nevertheless, for KIBs, alloying-type anodes have not been investigated frequently. Sn could make various alloys with K in the binary phase diagram as a frequently researched anode with impressive function in NIBs and LIBs, indicating the possible use of Sn and Sn-based materials in KIBs. Sultana et al. recently stated a 150 mAh/g capacity for Sn-based nanocomposite anodes in KIBs, albeit with a rapid decline in capacity. Moreover, for Sn anodes in KIBs, a complete description of the degradation and reaction method has not been published. For the production of Sn and other alloying-type anodes for high-function KIBs, a thorough understanding is necessary. An analysis of the electro-chemical function, degradation, and reaction methods of Sn nanoparticles in KIBs applying electrochemical in situ Transmission Electron Microscopy (TEM) testing is mentioned in this paper by using computer simulation, which offers a complete approach to learn the basic science of KIB alloy-type anodes. For KIBs, Sn nanoparticles offer a high capacity of 197 mAh/g but easily decay. In situ TEM, electrochemical research shows that Sn nanoparticles' electrochemical potassium ion occurs in a two-step process with KSn alloy emerging after complete reaction, while during de-potassiation, nanostructured pores development is completely recoverable during cycling. However, in a few cycles, substantial pulverization happens in the anodes, negatively affecting stability in the cycle. Computer simulation is considerably used to support the control and production planning as the main parts of the digital company. The simulation enables the imitation of a suggested solution to delineate the parameters of a system to gain the needed goals. For companies, simulation is to raise the specific processes and management, also it helps to imitate the efficiency, process in production area etc. The software solution works by the proposal of conceptual model with the related data. After that, a mathematical–logical model was generated that is served as a direct base for realization of simulation model. The behavior and structure of suggested entities need to imitate those of real objects and of the whole system. Subsequently, the realized logical model could be reflected into the selected simulation software. The generation of simulation model is based on the method that is closely related to the selected software solution.

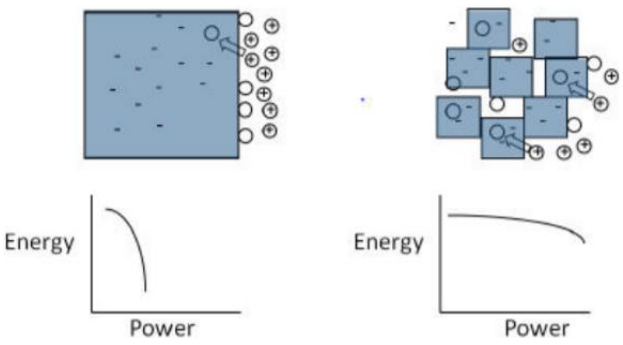

Fig. 3 Chemical reaction and energy/power balance of standard battery vs. Nano phosphate battery

Metal oxides (SnO_2, TiO_2, MoO_2, etc.) have the benefits of environmental friendliness, plentiful natural sources, and high theoretical particular capability as a promising anode material for alkali metal ion batteries. In the past few years, they have gained the interest of significant number of researchers. SnO_2, an essential member of metal oxides, was researched for LIBs and Sodium Ion Batteries (SIBs) as an anode element. However, fewer studies have been done to date on the K storage efficiency of SnO_2. It should be noted that SnO_2 has the drawbacks of less conductivity, weak reversibility and large volume change that have a significant effect on its reversible specific capacity and cycle stability, therefore affecting its practical value. The researchers improve SnO_2 with a conductive material (carbon material) or design special structures by new methods of synthesis to solve the above shortcomings in order to achieve excellent electrochemical efficiency. The carbon material will have a decent conductive network to increase the electronic conductivity of the overall electrode and to buffer the volume changes of SnO_2 along the electrode. While the methods above have significantly improved the electrochemical efficiency of SnO_2, there are still a number of issues with the practical application of SnO_2. The SnO_2 composites are generally combined with a conductive agent and a binder for coating on the metal current collector to act as the battery electrode for traditional powder electrode material. As a result, the inactive components substantially decrease the energy efficiency of the battery (current collectors and binders). Furthermore, the contact area of the traditional electrode between active material and electrolyte is small that is not conducive to the maximum application of the active material. In the end, in a repeated cycling process, the enormous volume changes of SnO_2 electrode resulted in electrode pulverization and escape, leading to rapid decay of capability and low performance. Consequently, it could be an impressive method of enhancing the overall function of SnO_2 to build binder-free, freestanding three-dimensional (3D) electrodes. In this research, as a freestanding anode for K storage, we anchor SnO_2 nanoparticles on 3D carbon foam (SnO_2@CF) via a simple electrodeposition process. The freestanding SnO_2@CF electrode obtained possesses a 3D conductive network, a large electrolyte contact area and supported K+ transfer. SnO_2@CF takes significant specific capacity, excellent cycle stability and rate performance in PIBs, benefiting from the above mentioned characteristics. In addition, via ex-situ XPS, XRD and TEM, the phase transition of SnO_2@CF during charge and discharge processes is seen. Nano batteries are manufactured batteries which use nanoscale method, a scale of minuscule particles measuring less than 100 nanometers or 10^{-7} meters. The anode is almost always graphite, so the cathode and electrolyte materials are often researched (Shah *et al.* 2016a, Nosrati *et al.* 2018). Higher conductivity can be accomplished by shrinking the size of the materials included in a Nano battery, resulting an improved power, both in charge and discharge (Shariati *et al.* 2011, Shah *et al.* 2015, Ziaei-Nia *et al.* 2018, Habibi *et al.* 2019b). Some technologies are predominantly used in Nano batteries: 1) Nano phosphate technology 2) Nano pore battery technology and 3) Lithium ion battery technology (using lithium titanate). An advanced battery system's overall performance and reliability is highly dependent on the chemistry used in the cell (Arabnejad Khanouki *et al.* 2010, 2011, Ismail *et al.* 2018). It is not necessary to mistake nano phosphate with regular lithium iron phosphate (LFP), which has a less capacity and power rate. Nano phosphate is a cathode of lithium ion batteries developed by Professor Todming Chiang and his team (Jalali *et al.* 2012, Davoodnabi *et al.* 2019, Xie *et al.* 2019). The particles of Nano phosphate are classified into two sets, i.e., Primary and also secondary. Chemical reactions provided by monophosphate technology, on the other hand, raise the cathode surface area of the electrolyte, allowing faster incorporation of lithium and leading to more power (Wei *et al.* 2018). Also, much of the bulk volume is still applied to store resources.

The persistent power capacity over a wide span of states of charge is another important aspect of Nano phosphate technology (SOC) (Mohammadhassani *et al.* 2014a, Li *et al.* 2019, Luo *et al.* 2019). At low SOC, majority of battery technologies have considerably lower power capabilities. Nano phosphate has outstanding abuse properties. Both of the lithium ions are moved throughout the full charge/discharge case in these chemistries (Hamidian *et al.* 2011, Shariati *et al.* 2018, 2019b). In majority of cathode metal oxide materials, particularly materials based on cobalt and nickel, only half of the lithium available is moved along normal activity (Shariati *et al.* 2010, Shah *et al.* 2016b, Shahabi *et al.* 2016). Since metallic lithium is far more reactive than ionic lithium, the consequence is that the lithium plates on the anode's surface produce risks (Daie *et al.* 2011, Mohammadhassani *et al.* 2014c, Nasrollahi *et al.* 2018). Since all the lithium ions in nano phosphate chemistry are transferred during charging to anode, during an overcharge case, it is far less common for lithium metal to plate on the anode surface (Afsar Dizaj *et al.* 2018, Al Kajbaf *et al.* 2018, Asadolahi *et al.* 2020, Rouhanifar *et al.* 2020). Usually, cycle life is characterized as the number of incidents a battery could be discharged and charged until its capacity falls below 70 to 80% of its original capacity or energy from the nameplate (Fanaie *et al.* 2014, 2015, 2016). Earlier, by positioning two electrodes inside a nanopore (made of anodic aluminum oxide) and utilizing ultra-thin electrical insulating material to isolate them, researchers

created 3-D nanostructured batteries (Goudarzi *et al.* 2016, Jahanbakhti *et al.* 2017, Ghanbari-Ghazijahani *et al.* 2020). This device has enhanced power and energy density, utilizing these thin electrical insulators restricts the retention of charge and involves complex circuits to transfer current between them (Qi *et al.* 2019, Majedi *et al.* 2020, Qi *et al.* 2020). However, due to spatial constraints of the material, it is hard to maintain the advantages of the 3-D nano-architecture. Liquid formulas of electrically conductive ions (electrolytes) were applied to connect battery circuits, rather than using wired circuits. On the other hand, nano-batteries that apply electrolytes displayed low charge storage (Ngo *et al.* 2018, Alaskar *et al.* 2020b, Cao *et al.* 2020c, Majedi *et al.* 2021). Additionally, uneven ion concentration gradients were led to uneven current densities when used in combination with 3-D structures. Recently, via the design of a battery that incorporates many components more efficiently, researchers have addressed these constraints (Han *et al.* 2018, Dinh-Cong *et al.* 2019, Alyousef *et al.* 2020, Huang *et al.* 2020). A parallel set of Nano batteries make up the latest battery design. All nanotubes include electrodes and liquid electrolytes situated in a nanopores made of anodic aluminum oxide. Each nanotube consisted of a current collector made as the energy storage material by an outside nanotube of an inner nanotube of V_2O_5. Every end of the nanopore was either coated with V_2O_5 or with a chemically changed form of V_2O_5 to act as the cathode and anode electrodes (Alaskar *et al.* 2020a, Cao *et al.* 2020a, d, Chowdhury 2021). The output of both individual electrodes was calculated. Both implementations demonstrated excellent preservation of electrical storage and a long lifetime charge-discharge cycle. This nanopore battery has triple the electrical storage capacity and an order of magnitude longer cycle life in comparison to prior nanowire battery devices utilizing the same material. The superior cycle lifetime is attributed by researchers to the coaxial tubular structure. The design of the nanotube was found to have a far higher electrical storage potential than the planar structure. These authors have shown that appropriately scaled nanostructures are a viable alternative for enhanced structures of batteries. This unique structure could be a choice for potential portable devices, including phones, tablets, and more, with an improved discharge lifetime and cycle lifetime.

2. Nano-structured battery

The specifications such as longer life, stability, remote UPS (uninterruptible power supply) applications are not fulfilled by lead-acid battery technology, and traditional Li-ion technology. Furthermore, abusive conditions such as short circuit, over recharge, exposure to excessively high or low temperatures, over discharge could not be tolerated by these technologies. Using nanotechnology, ALTAIRNANO designed a novel battery and reducing certain disadvantages of traditional designs. The Li-ion technology of ALTAIRNANO is different from the widely applied Li-ion model. They substituted the graphite material with nano-structured lithium titanate that is used in traditional batteries.

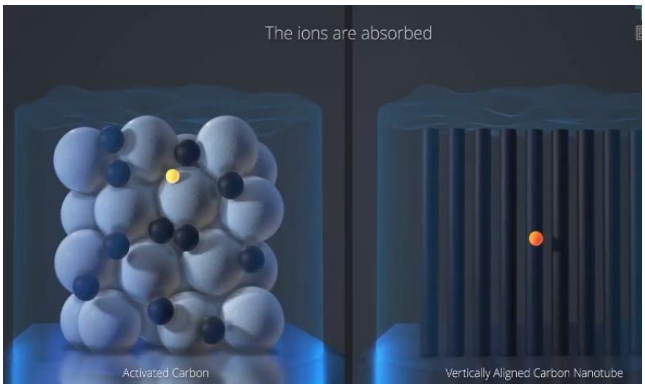

Fig. 4 Traditional Li-ion technology

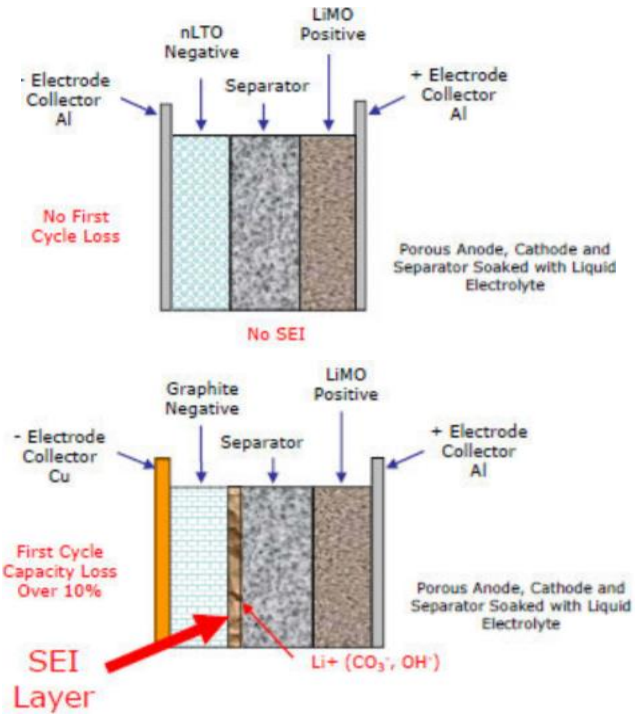

Fig. 5 Comparing of Nano structured battery (Fig. 1) and traditional graphite

3. Methodology preparation of SnO_2/SSM

A hydrothermal process was used to produce the SnO_2/SSM products. Especially, to ready the precursor solution, NaOH (1.2 g) and $SnCl_2{\cdot}2H_2O$ (3.4 g) were added at room temperature in 40 mL deionized (DI) water. The SSM was applied to the hydrothermal reaction precursor solution after ultrasound washing in dilute hydrochloric acid, DI water, ethanol and acetone, respectively. The mix has been moved into an autoclave of Teflon-lined stainless-steel and cooked (24 h) at 200°C. After treating the SSM with ethanol and DI water (5 times), SnO_2/SSM was extracted. During the processing of SnS_2/SnO_2/SSM, they were acquired by partial hydrothermal phase while vulcanizing SnO_2/SSM. In general, 1.1 g of thioacetamide (0.5 M) was dissolved in DI water (30 ml) and treated to form a homogeneous precursor solution with magnetic stirring (30 min). Then the precursor solution and SnO_2/SSM mixture were moved to an autoclave of Teflon-lined

stainless steel and reacted (24 hours at 180°C). The SnS_2/SnO_2/SSM products were finally collected.

4. Materials characterization

To have the morphology details of the items, scanning electron microscopy (SEM, FEI Verios 460) was used. Transmission electron microscopy (TEM, FEI Tecnai G2 F20 S-TWIN) equipped with energy-dispersive X-ray spectroscopy has identified the crystal structure of the samples (EDS). In order to gather the XRD patterns of the items, the D/max2200PC X-Ray diffractometer with CuK ax radiation was used. photoelectron spectroscopy (XPS) instrument Axis Ultra X-ray. Was used to record the chemical state of elements was recorded.

5. Electrochemical measurements

Electrochemical measurements by CR2032-type coin cells were performed by computer simulation to determine the potassium storage performance of the items. SnS_2/SnO_2-SSM was utilized as a working electrode to assemble the cells, and both counter and reference electrodes were used for the potassium metal. The mean mass load of active materials was determined before and after the hydrothermal reaction phase by measuring the weight of SSM substrate. The density of loading for active materials is approximately 1.2, and for SnO_2/SSM, SnS_2/SnO_2/SSM, 1.0 mg cm-2. The electrolyte was a 1 M KPF6 nonaqueous solution in a 1:1 (v/v) ethylene carbonate (EC) and diethyl carbonate mixture (DEC). Glass fiber (GF/D) from Whatman are the separators in this study. In a glove box packed with high-purity argon, the cells were assembled. The galvanostatic charge and discharge method was recorded at ambient temperature at various densities using the LAND-CT2011A device. The Cyclic Voltammetry (CV) curves were gained through an electrochemical workstation (CHI600E). A hydrothermal method was used to prepare the SnO_2 nanosheets/SSM materials. 1.2 g NaOH and 3.4 g $SnCl_2{\cdot}_2H_2O$ (0.38 M) were dissolved in 40 mL ultrapure water at ambient temperature in a standard procedure to form a homogeneous precursor solution for 30 minutes under magnetic stirring. SSM was ultrasonically washed prior to being added to the above precursor in dilute hydrochloric acid, deionized water, ethanol and acetone, respectively. The mixture was then put in an autoclave of Teflon-lined stainless steel and heated in an oven for 24 h at 200°C and then naturally cooled at ambient temperature. SnO_2 nanosheets/SSM obtained were rinsed with ethanol ultrapure and water, then dried in the ambient atmosphere overnight at 80°C. SnO_2/SSM samples with a $SnCl_2$ concentration of 0.2 M and 0.56 M have also been collected for comparison, although other conditions remain the same. On a D/max2200PC X-ray diffractometer with Cu K Al radiation, X-ray diffraction (XRD) patterns were recorded. X-ray photoelectron spectroscopy was utilized to determine the surface chemical state of the elements (XPS, AXIS SUPRA). The CR2032-type coin cells were used to perform

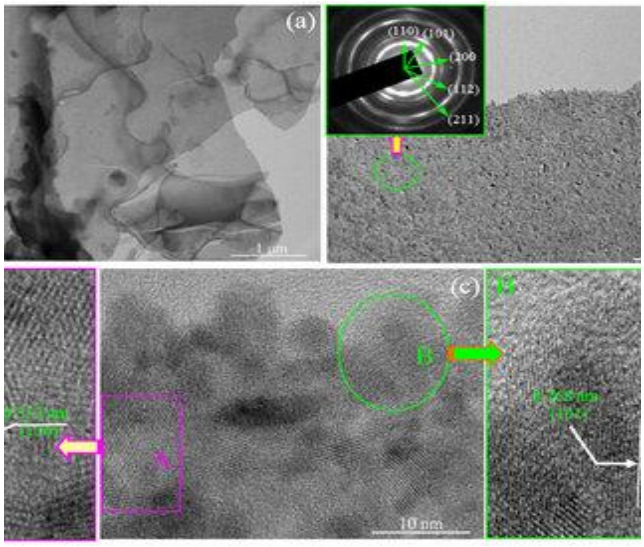

Fig. 6 SnO_2 Nano sheets, synthesis, characterization and structure

electrochemical measurements. The as-synthesized SnO_2/SSM was the working electrode and the potassium metal acted as reference electrodes and the counter via simulation. Before and after SnO_2 was produced, the mass loading of SnO_2 was gained by weighing specific SSM substrates. On average, for SnO_2/SSM-1, SnO_2/SSM-2 and SnO_2/SSM-3 the loading density of SnO_2 is 0.4, 1.6 and 3.8 mg cm^{-2}. As an electrolyte, a 1 M KPF6 nonaqueous solution was used in a 1:1 (v/v) mixture of ethylene carbonate (EC) and diethyl carbonate (DEC). Whatman's glass fiber (GF/D) was used as the dividers. They assembled and disassembled the coin cells in an argon-filled glove box. Using the LAND-CT2011A battery-testing instrument at ambient temperature, the coin cells were galvanostatically discharged and charged at various densities in a voltage spane of 0.01-2.6 V. An electrochemistry workstation estimated CVs scanned at a voltage window of 0.01-2.5 V at 0.1 mV s^{-1} (CHI618D).

6. Result and discussion

The high and low magnification SEM images of SnO_2/SSM samples was ready with various concentrations of $SnCl_2$ are illustrated in Fig. 8. From Figs.7(a)-(c), it could be shown that the metal wires were about 40 μm in diameter. It was seen that as the concentration of $SnCl_2$ raised, the load of SnO_2 nanostructures slowly increased. Small Nano sheets less than 10 nm in size were grown on the SSM surface when the $SnCl_2$ concentration was 0.2 M, as shown in Fig. 7(d). Wide Nano sheets with a size of roughly 800 nm were collected on the SSM surface when the $SnCl_2$ concentration was increased to 0.38 M, as shown in Fig. 7(d).

It is possible to relate the formation of Nano sheets to the directed attachment of SnO_2 nanoparticles that shaped at the early phase of reactions. Because of more electrolyte contact area and short ion diffusion duration, these large

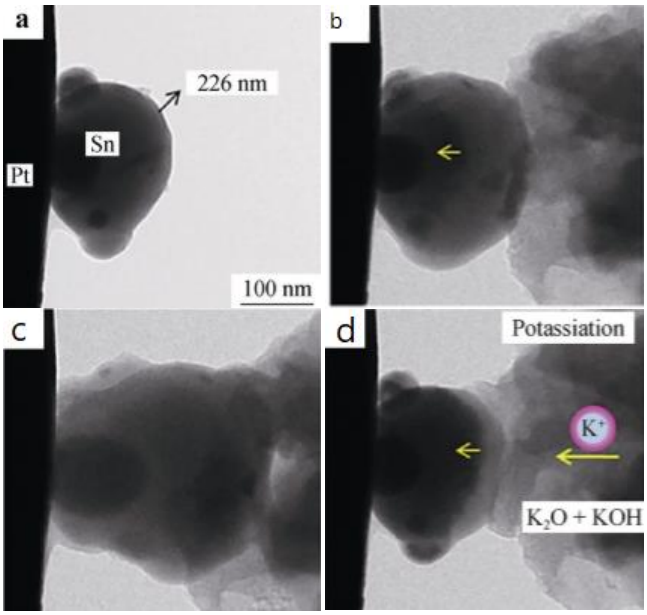

Fig. 7 (a) a pristine Sn nanoparticle; (b) first-step potassiat ion procedure, where arrows reflect path of K+ diffusion; (c) second-step potassiat ion process, without a definite boundary; (d) first-step potassiat ion process, where arrows show direction of K+ diffusion

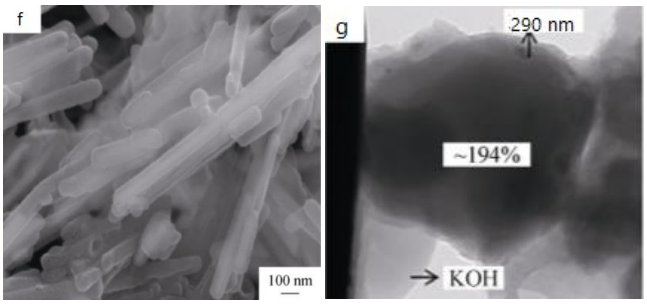

Fig. 8 SEM image and b TEM image; electrochemical performances of Sb@HCT as anode for PIBs: c cycling performance

size Nano sheets prefer high capacity in KIB electrodes. In Fig. 8(g), it can be shown that the film covered by large crystal particles on the surface of SSM increased to 0.48 M after the concentration of $SnCl_2$. As $SnCl_2$ concentration raised from 0.2 M to 0.48 M, the morphologies of SnO_2 changed from small Nano sheets by large Nano sheets to large crystal particles. The method of producing of the integrated SnS_2/SnO_2/SSM flexible binder-free electrodes is outlined in Fig. 7. Initially, by hydrothermal technique, SnO_2 nano sheets were grown on SSM to obtain SnO_2/SSM (stage I). Subsequently, a hydrothermal vulcanization procedure through thioacetamide as a sulfur source (stage II) was performed on SnO_2/SSM. Finally, uniformly textured SnS_2/SnO_2 hetero structured Nano sheets have been obtained on the SSM surface.

The SnO_2/SSM and SnS_2/SnO_2/SSM SEM images are shown in Figs. 7(a)-(d). The Nano sheets are ultra-thin with a grapheme-like morphology after the vulcanization process, as shown in Fig. 7(d). When tested as an alkali metal ion battery anode, the ultra-thin morphology can provide a large electrolyte interface area. SnO_2 and

Table 1 Physical/electrochemical features and economic factors of lithium, sodium, and potassium

Physical/electrochemical properties/economic parameters	Li	Na	K
Atomic number	3	11	9
Atomic mass, u	6.941	22.989	39.098
Density, g cm^{-3}	0.535	0.968	0.856
Melting point, °C	180.45	97.72	63.38
Atomic radius, pm	145	180	220
Ionic radius, Å	0.76	1.02	1.38
Covalent radius, pm	128	166	203
Electronic shell structure	(1, 2)	(1, 2, 8)	(1, 2, 8)
Electronic configuration	(He) $2s^1$	(Ne) $3s^1$	(Ar) $4s^1$
Voltage vs SHE, V	−3.04	−2.71	−2.93
Theoretical capacity of the metal electrode, mAh g^{-1}	3861	1166	685
Crust abundance, mass %	0.0017	2.3	1.5
Crust abundance, molar %	0.005	2.1	0.78
Cost of carbonate, US$ ton^{-1}	6500	200	1000
Cost of industrial-grade metal, US$ ton^{-1}	100 000	3000	13 000

SnS_2/SnO_2, TEM images are shown in Fig. 6. It is possible to see that SnS_2/SnO_2 was seen as ultra-thin Nano sheets and rolled up some edges of SnS_2/SnO_2 Nano sheets, further suggesting the graphene-like morphology. In Fig. 7(b), it can be seen that the mapping of SnS_2/SnO_2 by energy-dispersive X-ray spectrometry (EDX) and the uniform distribution of Sn, O and S elements can be seen across the entire Nano layer. The SnS_2/SnO_2 high-resolution transmission electron microscopy (HRTEM) image is shown in Fig 7(c). It is possible to align the crystalline fringes with space distances of 0.48 nm and 0.26 nm (Fig. 7(d)) with the (001) SnS_2 and (101) SnO_2 planes, respectively, suggesting that the partial SnO_2 phase has been successfully converted to SnS_2 phase. It is possible to clearly see the interface of SnS_2 and SnO_2, as shown in Fig. 7(c), which is desirable for the movement of electrons along electrochemical reactions. Also, the phase compositions of the SnS_2/SnO_2/SSM products, XRD characterization was applied and the XRD pattern is illustrated in Fig. 8(f). The peaks diffracted at 2θ of 43.6° and 50.8° were indexed to SSM substrate. As shown in Fig. 8(g), new peaks were seen at 2θ of 32.1°, 41.8° and 49.9°, which are well indexed with the (101), (102) and (110) planes of SnS_2. In order to acquire further knowledge about the chemical states on the SnS_2/SnO_2/SSM surface products, XPS was utilized. The standard range of an XPS survey in Fig. 8 demonstrates the existence of C, Sn, S and O, where the origin of element C is the adsorbed gaseous molecules. Using the elements composition presented in Table 1 which were extracted from XPS survey spectrum, the compositions of SnO_2 and SnS_2 are computed to be ca. 40 wt% SnO_2 and 60 wt% SnS_2

respectively. Figs. 7(b)-(d) shows the high resolution XPS spectra of Sn 3d, O 1s and S 2p. The peaks at 484.6 eV and 493.2 eV in Fig. 7(b) are adjusted to Sn 3d3/2 and Sn 3d5/2 peaks. The binding energy of O 1 s in Fig. 7(c) is 532.2 eV, referring to Sn-O bonding's binding energy. The C-O and O-H bonds, which could be linked to the absorbed gaseous and H_2O molecules, which can stem from the convoluted peaks at 533.9 and 530.0 eV. Via cyclic voltammetry (CV) and galvanostatic charge/discharge checking, the potassium storage properties of the SnS_2/ SnO_2/SSM were assessed. Two pronounced cathodic peaks are observed at 0.64 and 1.51 V in the starting cycle for the SnS_2/SnO_2/SSM electrode relative to the CVs of the SnO_2/SSM electrode, and then disappeared in the second and third cycles. The irreversible reactions and the presence of a stable solid-electrolyte interphase (SEI) film on the surface of SnS_2/SnO_2 may be related to the inconsistency of CV curves. With almost complete overlapping, the subsequent cycles present strong reversibility, suggesting high reversibility during the reaction. The peak at 0.79 V can be assigned to forming the KxSn alloys in the second cathodic scanning. While the peaks at 1.16 and 1.56 V may be due to the multistep de-alloying process of KxSn in the second anodic scanning. The SnS_2/SnO_2/SSM electrode galvanostatic charge/discharge curves at 50 mA g^{-1} are shown in Fig. 8(f). 722 mAh g^{-1} and 474 mAh g^{-1} are the discharge and charge capacities for the first cycle with a coulombic efficiency (CE) of 65.6%. Due to the reduced electrochemical resistance, SEI formation can play a critical part in obtaining a high CE after the initial cycle. The CE is, therefore, rising after the initial five cycles. For the 50th cycle, the charge and discharge power is 398 and 400 mAh g^{-1} with a 99% higher CE. It can be seen that throughout the entire cycles, SnS_2/SnO_2/SSM tends to be greater than SnO_2/SSM in terms of capacity. The discharge capacity of SnS_2/SnO_2/SSM can be maintained at 391 mAh g^{-1} after 100 cycles, while the capacity of SnO_2/SSM is 300 mAh g^{-1}. On the basis of the 45 wt% SnO_2 and 50 wt% SnS_2 composition in the SnS_2/SnO_2/SSM, it can be inferred that SnS_2 and SnO_2 provide capacities of approximately 250 mAh g^{-1} and 125 mAh g^{-1}, respectively.

7. Conclusions

This study has focused on the economic and management use of rhododendron petals in potassium-ion Nano batteries anode via efficient Computer simulation. In this case, freestanding SnO_2/SSM composites have been engineered and prepared as anode materials for PIBs. Freestanding SnO_2/SSM composites were designed as anode materials for PIBs. They anchored the SnO_2 nanoparticles. Researches on performance improvement strategies and failure mechanisms of SnO_2 anode in full cell LIBs should be prioritized in order to realize the realistic application of SnO_2 in next generation LIBs with higher energy density, longer lifetime, higher protection, faster charge/discharge rate, and lower price. The low initial Coulombic efficiency is by far the most important concern of SnO_2 anodes in full cells (CE). Aside from low electrical conductivity, large volume expansion and slow reaction kinetics, the key explanations for the seen degradation of reaction reversibility and power decay of SnO_2 are not as obvious as those of LIBs as anodes of SIBs and KIBs (i.e., coarsening of Sn NPs). The engineered synthesis of SnO_2-based materials with optimal structures and components with high capacity and long life as anodes of SIBs and KIBs will direct the uncovering of these mechanisms. SnO_2-based materials, however, have been thoroughly reviewed as anodes for batteries of Li-ion and Na-ion. Electrode technologies have been investigated to a reasonably mature stage for Li-ion batteries with recent material problems focusing primarily on protection, energy density and cost reduction by computer simulation. Electrode materials for Na-ion batteries are still under development, and electrode materials, particularly negative materials, should be further improved to meet the requirements for economically viable anode Na-ion batteries. In addition, various methods can boost the electrochemical efficiency of electrode materials, including growing electronic conductivity, shrinking the duration of ion diffusion, changing microstructures, and compositing with carbonaceous materials.

References

Afshar, A., Jahandari, S., Rasekh, H., Shariati, M., Afshar, A. and Shokrgozar, A. (2020), "Corrosion resistance evaluation of rebars with various primers and coatings in concrete modified with different additives", *Constr. Build. Mater.*, **262**, 120034. https://doi.org/10.1016/j.conbuildmat.2020.120034.

Afsar Dizaj, E., Fanaie, N. and Zarifpour, A. (2018), "Probabilistic seismic demand assessment of steel frames braced with reduced yielding segment buckling restrained braces", *Adv. Struct. Eng.*, **21**(7), 1002-1020. https://doi.org/10.1177%2F1369433217737115.

Al Kajbaf, A., Fanaie, N. and Najarkolaie, K.F. (2018), "Numerical simulation of failure in steel posttensioned connections under cyclic loading", *Eng. Fail. Anal.*, **91**, 35-57. https://doi.org/10.1016/j.engfailanal.2018.04.024.

Alaskar, A., Shah, S., Keerio, M.A., Phulpoto, J.A., Baharom, S., Assilzadeh, H., Alyousef, R., Alabduljabbar, H. and Mohamed, A.M. (2020a), "Development of Pozzolanic material from clay", *Adv. Concrete Construct., Int. J.*, **10**(4), 301-310. https://doi.org/10.12989/acc.2020.10.4.301.

Alaskar, A., Wakil, K., Alyousef, R., Jermsittiparsert, K., Ho, L. S., Alabduljabbar, H., Alrshoudi, F. and Mohamed, A.M. (2020b), "Computational analysis of three dimensional steel frame structures through different stiffening members", *Steel Compos. Struct., Int. J.*, **35**(2), 187-197. https://doi.org/10.12989/scs.2020.35.2.187.

Alyousef, R., Alabduljabbar, H., Mohamed, A.M., Alaskar, A., Jermsittiparsert, K. and Ho, L.S. (2020), "A model to develop the porosity of concrete as important mechanical property", *Smart Struct. Syst., Int. J.*, **26**(2), 147-156. https://doi.org/10.12989/sss.2020.26.2.147.

Arabnejad Khanouki, M.M., Ramli Sulong, N.H. and Shariati, M. (2010), "Investigation of seismic behaviour of composite structures with concrete filled square steel tubular (CFSST) column by push-over and time-history analyses", *Proceedings of the 4th International Conference on Steel and Composote Structurees.* http://doi.org/10.3850/978-981-08-6218-3_CC-Fr003.

Arabnejad Khanouki, M.M., Ramli Sulong, N.H. and Shariati, M. (2011), "Behavior of through beam connections composed of CFSST columns and steel beams by finite element studying",

Adv. Mater. Res., **168**, 2329-2333. http://doi.org/10.4028/www.scientific.net/AMR.168-170.2329.

Asadolahi, S.M. and Fanaie, N. (2020), "Performance of self-centering steel moment frame considering stress relaxation in prestressed cables", *Adv. Struct. Eng.*, 1369433219900940. https://doi.org/10.1177%2F1369433219900940.

Baumann, M., Domnik, T., Haase, M., Wulf, C., Emmerich, P., Rösch, C., Zapp, P., Naegler, T. and Weil, M. (2021), "Comparative patent analysis for the identification of global research trends for the case of battery storage, hydrogen and bioenergy", *Technol. Forecast. Social Change*, **165**, 120505. https://doi.org/10.1016/j.techfore.2020.120505.

Cao, Y., Alyousef, R., Baharom, S., Shah, S., Alaskar, A., Alabduljabbar, H., Mustafa Mohamed, A. and Assilzadeh, H. (2020a), "Dynamic attainment of mixed aspect ratio for concrete members reinforced with steel fiber under impact loading", *Mech. Adv. Mater. Struct.*, 1-10. https://doi.org/10.1080/15376494.2020.1847371.

Cao, Y., Fan, Q., Azar, S.M., Alyousef, R., Yousif, S.T., Wakil, K., Jermsittiparsert, K., Ho, L.S., Alabduljabbar, H. and Alaskar, A. (2020b), "Computational parameter identification of strongest influence on the shear resistance of reinforced concrete beams by fiber reinforcement polymer", *Structures*, **22**. https://doi.org/10.1016/j.istruc.2020.05.031.

Cao, Y., Wakil, K., Alyousef, R., Jermsittiparsert, K., Ho, L.S., Alabduljabbar, H., Alaskar, A., Alrshoudi, F. and Mohamed, A.M. (2020c), "Application of extreme learning machine in behavior of beam to column connections", *Structures*, **25**. https://doi.org/10.1016/j.istruc.2020.03.058.

Cao, Y., Wakil, K., Alyousef, R., Yousif, S.T., Jermsittiparsert, K., Ho, L.S., Alabduljabbar, H., Alaskar, A., Alrshoudi, F. and Mohamed, A.M. (2020d), "Computational earthquake performance of plan-irregular shear wall structures subjected to different earthquake shock situations", *Earthq. Struct. Int. J.*, **18**(5), 567-580. https://doi.org/10.12989/eas.2020.18.5.567.

Chahnasir, E.S., Zandi, Y., Shariati, M., Dehghani, E., Toghroli, A., Mohamed, E.T., Shariati, A., Safa, M., Wakil, K. and Khorami, M. (2018), "Application of support vector machine with firefly algorithm for investigation of the factors affecting the shear strength of angle shear connectors", *Smart Struct. Syst., Int. J.*, **22**(4), 413-424. http://doi.org/10.12989/sss.2018.22.4.413.

Chen, Y., He, L., Li, J. and Zhang, S. (2018), "Multi-criteria design of shale-gas-water supply chains and production systems towards optimal life cycle economics and greenhouse gas emissions under uncertainty", *Comput. Chem. Eng.*, **109**, 216-235. https://doi.org/10.1016/j.compchemeng.2017.11.014.

Chen, C., Shi, L., Shariati, M., Toghroli, A., Mohamad, E.T., Bui, D.T. and Khorami, M. (2019), "Behavior of steel storage pallet racking connection-A review", *Steel Compose. Struct., Int. J.*, **30**(5), 457-469. https://doi.org/10.12989/scs.2019.30.5.457.

Chen, M.-J., Nguyen, D.Q.A. and Tran, T.C. (2020), "ZnO nanoarticles in bettering the color uniformity of phosphor-converted white LED lights", *J. Adv. Eng. Computat.*, **4**(3), 173-180. http://doi.org/10.25073/jaec.202043.280.

Cheng, F., Chen, J., Gou, X. and Shen, P. (2005), "High-power alkaline Zn–MnO_2 batteries using γ-MnO_2 nanowires/nanotubes and electrolytic zinc powder", *Adv. Mater.*, **17**(22), 2753-2756. https://doi.org/10.1002/adma.200500663.

Chernogorov, I., Polyakh, V. and Yarakhmedov, O. (2017), "Search optimization opportunities of modified self-organizing migrating algorithm in multi-extremal tasks environment", *J. Adv. Eng. Computat.*, **1**(2), 144-152. http://doi.org/10.25073/jaec.201712.60.

Choi, Y., Jung, B., Lee, D., Jeong, J., Kim, K., Ahn, H., Cho, K. and Gu, H. (2007), "Electrochemical properties of sulfur electrode containing nano Al_2O_3 for lithium/sulfur cell", *Physica Scripta*, **2007**(T129), 62. http://doi.org/10.1088/00318949/2007/T129/014.

Chowdhury, I.A. (2021), "Performance Analysis of a SWIPT Enabled UAV-Assisted Relaying", *J. Adv. Eng. Computat.*, **5**(1), 19-26. http://doi.org/10.25073/jaec.202151.310.

Daie, M., Jalali, A., Suhatril, M., Shariati, M., Arabnejad Khanouki, M.M., Shariati, A. and Kazemi-Arbat, P. (2011), "A new finite element investigation on pre-bent steel strips as damper for vibration control", *Int. J. Phys. Sci.*, **6**(36), 8044-8050. https://doi.org/10.5897/ijps11.1585.

Davoodnabi, S.M., Mirhosseini, S.M. and Shariati, M. (2019), "Behavior of steel-concrete composite beam using angle shear connectors at fire condition", *Steel Compos. Struct., Int. J.*, **30**(2), 141-147. https://doi.org/10.12989/scs.2019.30.2.141.

Dinh-Cong, D., Keykhosravi, M.H., Alyousef, R., Salih, M.N., Nguyen, H., Alabduljabbar, H., Alaskar, A., Alrshoudi, F. and Poi-Ngian, S. (2019), "The effect of wollastonite powder with pozzolan micro silica in conventional concrete containing recycled aggregate", *Smart Struct. Syst., Int. J.*, **24**(4), 541-552. https://doi.org/10.12989/sss.2019.24.4.541.

Douglas, A., Carter, R., Oakes, L., Share, K., Cohn, A.P. and Pint, C.L. (2015), "Ultrafine iron pyrite (FeS2) nanocrystals improve sodium–sulfur and lithium–sulfur conversion reactions for efficient batteries", *ACS Nano*, **9**(11), 11156-11165. https://doi.org/10.1021/acsnano.5b04700.

Dyatlov, S., Didenko, N., Ivanova, E., Soshneva, E. and Kulik, S. (2020), "Prospects for alternative energy sources in global energy sector", In *IOP Conference Series: Earth Environ. Sci.*, IOP Publishing. http://doi.org/10.1088/1755-1315/434/1/012014.

Fanaie, N. and Ezzatshoar, S. (2014), "Studying the seismic behavior of gate braced frames by incremental dynamic analysis (IDA)", *J. Construct. Steel Res.*, **99**, 111-120. https://doi.org/10.1016/j.jcsr.2014.04.008.

Fanaie, N., Esfahani, F.G. and Soroushnia, S. (2015), "Analytical study of composite beams with different arrangements of channel shear connectors", *Steel Compos. Struct., Int. J.*, **19**(2), 485-501. https://doi.org/10.12989/scs.2015.19.2.485.

Fanaie, N., Aghajani, S. and Afsar Dizaj, E. (2016), "Strengthening of moment-resisting frame using cable–cylinder bracing", *Adv. Struct. Eng.*, **19**(11), 1736-1754. https://doi.org/10.1177%2F1369433216649382.

Fujita, T., Chen, H., Wang, K.T., He, C.L., Wang, Y.B., Dodbiba, G. and Wei, Y.Z. (2021), "Reduction, reuse and recycle of spent Li-ion batteries for automobiles: A review", *Int. J. Miner., Metall. Mater.*, **28**(2), 179-192. https://doi.org/10.1007/s12613-020-2127-8.

Ghanbari-Ghazijahani, T., Nabati, A., Azandariani, M.G. and Fanaie, N. (2020), "Crushing of steel tubes with different infills under partial axial loading", *Thin Wall. Struct.*, **149**, 106614. https://doi.org/10.1016/j.tws.2020.106614.

Goudarzi, A., Ghassemieh, M., Fanaie, N., Laefer, D.F. and Baei, M. (2016), "Axial load effects on flush end-plate moment connections", *Proceedings of the Institution of Civ. Engineers-Structures and Buildings* **170**(3), 199-210. https://doi.org/10.1680/jstbu.15.00042.

Guo, L.-f., Zhang, S.-y., Xie, J., Zhen, D., Jin, Y., Wan, K.-y., Zhuang, D.-g., Zheng, W.-q. and Zhao, X.-b. (2020), "Controlled synthesis of nanosized Si by magnesiothermic reduction from diatomite as anode material for Li-ion batteries", *Int. J. Miner., Metall. Mater.*, **27**(4), 515-525. https://doi.org/10.1007/s12613-019-1900-z.

Habibi, M., Mohammadgholiha, M. and Safarpour, H. (2019a), "Wave propagation characteristics of the electrically GNP-reinforced nanocomposite cylindrical shell", *J. Brazil. Soc. Mech. Sci, Eng.*, **41**(5), 1-15. https://doi.org/10.1007/s40430-019-1715-x.

Habibi, M., Taghdir, A. and Safarpour, H. (2019b), "Stability analysis of an electrically cylindrical nanoshell reinforced with graphene nanoplatelets", *Compos. Part B-Eng.*, **175**, 107125. https://doi.org/10.1016/j.compositesb.2019.107125.

Hamidian, M., Shariati, M., Arabnejad, M. and Sinaei, H. (2011), "Assessment of high strength and light weight aggregate concrete properties using ultrasonic pulse velocity technique", *Int. J. Phys. Sci.*, **6**(22), 5261-5266. https://doi.org/10.5897/IJPS11.1081.

Han, Y., Liu, S.-y., Cui, L., Xu, L., Xie, J., Xia, X.-K., Hao, W.-K., Wang, B., Li, H. and Gao, J. (2018), "Graphene-immobilized flower-like Ni_3S_2 nanoflakes as a stable binder-free anode material for sodium-ion batteries", *Int. J. Miner. Metall. Mater.*, **25**(1), 88-93. https://doi.org/10.1007/s12613-018-1550-6.

He, M., Kravchyk, K., Walter, M. and Kovalenko, M.V. (2014), "Monodisperse antimony nanocrystals for high-rate Li-ion and Na-ion battery anodes: Nano versus bulk", *Nano Lett.*, **14**(3), 1255-1262. https://doi.org/10.1021/nl404165c.

Hou, H., Jing, M., Yang, Y., Zhu, Y., Fang, L., Song, W., Pan, C., Yang, X. and Ji, X. (2014), "Sodium/lithium storage behavior of antimony hollow nanospheres for rechargeable batteries", *ACS Appl. Mater. Interf.*, **6**(18), 16189-16196. https://doi.org/10.1021/am504310k.

Hu, Y., Chen, Q., Feng, S. and Zuo, C. (2020), "Microscopic fringe projection profilometry: A review", *Opt. Laser. Eng.*, 106192. https://doi.org/10.1016/j.optlaseng.2020.106192.

Huang, J., Alyousef, R., Suhatril, M., Baharom, S., Alabduljabbar, H., Alaskar, A. and Assilzadeh, H. (2020), "Influence of porosity and cement grade on concrete mechanical properties", *Adv. Concrete Construct., Int. J.*, **10**(5), 393-402. https://doi.org/10.12989/acc.2020.10.5.393.

Huang, X., Zhang, Y., Moradi, Z. and Shafiei, N. (2021), "Computer simulation via a couple of homotopy perturbation methods and the generalized differential quadrature method for nonlinear vibration of functionally graded non-uniform micro-tube", *Eng. Comput.*, 1-18. https://doi.org/10.1007/s00366-021-01395-7.

Iost, R.M., Crespilho, F.N., Kern, K. and Balasubramanian, K. (2016), "A primary battery-on-a-chip using monolayer graphene", *Nanotechnology*, **27**(29), 29LT01. https://doi.org/10.1088/0957-4484/27/29/29LT01.

Ismail, M., Shariati, M., Abdul Awal, A.S.M., Chiong, C.E., Sadeghipour Chahnasir, E., Porbar, A., Heydari, A. and khorami, M. (2018), "Strengthening of bolted shear joints in industrialized ferrocement construction", *Steel Compos. Struct., Int. J.*, **28**(6), 681-690. https://doi.org/10.12989/scs.2018.28.6.681.

Jahanbakhti, E., Fanaie, N. and Rezaeian, A. (2017), "Experimental investigation of panel zone in rigid beam to box column connection", *J. Construct. Steel Res.*, **137**, 180-191. https://doi.org/10.1016/j.jcsr.2017.06.025.

Jalali, A., Daie, M., Nazhadan, S.V.M., Kazemi-Arbat, P. and Shariati, M. (2012), "Seismic performance of structures with pre-bent strips as a damper", *Int. J. Phys. Sci.*, **7**(26), 4061-4072. 4061-4072. https://doi.org/10.5897/IJPS11.1324.

Kang, Y., Zhang, Y.-H., Shi, Q., Shi, H., Xue, D. and Shi, F.-N. (2021), "Highly efficient Co_3O_4/CeO_2 heterostructure as anode for lithium-ion batteries", *J. Coll. Interf. Sci.*, **585**, 705-715. https://doi.org/10.1016/j.jcis.2020.10.050.

Katebi, J., Shoaei-parchin, M., Shariati, M., Trung, N.-T. and Khorami, M. (2019), "Developed comparative analysis of metaheuristic optimization algorithms for optimal active control of structures", *Eng. Comput.*, 1-20. https://doi.org/10.1007/s00366-019-00780-7.

Kim, M.G., Sim, S. and Cho, J. (2010), "Novel core-shell Sn-Cu anodes for lithium rechargeable batteries prepared by a redox-transmetalation reaction", *Adv. Mater.*, **22**(45), 5154-5158. https://doi.org/10.1002/adma.201002480.

Kim, H., Kim, S.-W., Hong, J., Park, Y.-U. and Kang, K. (2011a), "Electrochemical and ex-situ analysis on manganese oxide/graphene hybrid anode for lithium rechargeable batteries", *J. Mater. Res.*, **26**(20), 2665. https://doi.org/10.1557/jmr.2011.301.

Kim, H., Seo, D.-H., Kim, S.-W., Kim, J. and Kang, K. (2011b), "Highly reversible Co_3O_4/graphene hybrid anode for lithium rechargeable batteries", *Carbon*, **49**(1), 326-332. https://doi.org/10.1016/j.carbon.2010.09.033.

Kim, S.-W., Lee, H.-W., Muralidharan, P., Seo, D.-H., Yoon, W.-S., Kim, D.K. and Kang, K. (2011c), "Electrochemical performance and ex situ analysis of $ZnMn_2O_4$ nanowires as anode materials for lithium rechargeable batteries", *Nano Res.*, **4**(5), 505-510. https://doi.org/10.1007/s12274-011-0106-0.

Lei, Z., Hao, S., Yang, J. and Dan, X. (2020), "Study on solid waste pyrolysis coke catalyst for catalytic cracking of coal tar", *Int. J. Hydrogen Energ.*, **45**(38), 19280-19290. https://doi.org/10.1016/j.ijhydene.2020.05.075.

Lei, Z., Hao, S., Yang, J., Zhang, L., Fang, B., Wei, K., Lingbo, Q., Jin, S. and Wei, C. (2021), "Study on denitration and sulfur removal performance of Mn–Ce supported fly ash catalyst", *Chemosphere*, **270**, 128646. https://doi.org/10.1016/j.chemosphere.2020.128646.

Li, H., Huang, X. and Chen, L. (1999), "Electrochemical impedance spectroscopy study of SnO and nano-SnO anodes in lithium rechargeable batteries", *J. Power Sources*, **81**, 340-345. https://doi.org/10.1016/S0378-7753(99)00214-1.

Li, D., Toghroli, A., Shariati, M., Sajedi, F., Bui, D.T., Kianmehr, P., Mohamad, E.T. and Khorami, M. (2019), "Application of polymer, silica-fume and crushed rubber in the production of Pervious concrete", *Smart Struct. Syst., Int. J.*, **23**(2), 207-214. https://doi.org/10.12989/sss.2019.23.2.207.

Liu, Y., Zhang, B., Xiao, S., Liu, L., Wen, Z. and Wu, Y. (2014), "A nanocomposite of MoO_3 coated with PPy as an anode material for aqueous sodium rechargeable batteries with excellent electrochemical performance", *Electrochimica Acta*, **116**, 512-517. https://doi.org/10.1016/j.electacta.2013.11.077.

Liu, C., Wu, X., Wakil, K., Jermsittiparsert, K., Ho, L.S., Alabduljabbar, H., Alaskar, A., Alrshoudi, F., Alyousef, R. and Mohamed, A.M. (2020), "Computational estimation of the earthquake response for fibre reinforced concrete rectangular columns", *Steel Compos. Struct., Int. J.*, **34**(5), 743-767. https://doi.org/10.12989/scs.2020.34.5.743.

Liu, Y., Wei, Z., Zhong, B., Wang, H., Xia, L., Zhang, T., Duan, X., Jia, D., Zhou, Y. and Huang, X. (2021), "O-, N-Coordinated single Mn atoms accelerating polysulfides transformation in lithium-sulfur batteries", *Energ. Storage Mater.*, **35**, 12-18. https://doi.org/10.1016/j.ensm.2020.11.011.

Lowy, D.A. and Patrut, A. (2008), "Nonobatteries: decreasing size power sources for growing technologies", *Recent Patent. Nanotechnol.*, **2**(3), 208-219. https://doi.org/10.2174/187221008786369642.

Luo, Z., Sinaei, H., Ibrahim, Z., Shariati, M., Jumaat, Z., Wakil, K., Pham, B.T., Mohamad, E.T. and Khorami, M. (2019), "Computational and experimental analysis of beam to column joints reinforced with CFRP plates", *Steel Compos. Struct., Int. J.*, **30**(3), 271-280. http://doi.org/10.12989/scs.2019.30.3.271.

Majedi, M., Afrazi, M. and Fakhimi, A. (2020), "FEM-BPM simulation of SHPB testing for measurement of rock tensile strength", *Proceedings of the 54th US Rock Mechanics/Geomechanics Symposium*, American Rock Mechanics Association. https://doi.org/12.2347/25103-35.4.

Majedi, M.R., Afrazi, M. and Fakhimi, A. (2021), "A micromechanical model for simulation of rock failure under high strain rate loading", *Int. J. Civ. Eng.*, **19**(5), 501-515.

https://doi.org/10.1007/s40999-020-00551-2.

Mansouri, I., Shariati, M., Safa, M., Ibrahim, Z., Tahir, M. and Petković, D. (2019), "Analysis of influential factors for predicting the shear strength of a V-shaped angle shear connector in composite beams using an adaptive neuro-fuzzy technique", *J. Intell. Manuf.*, **30**(3), 1247-1257. https://doi.org/10.1007/s10845-017-1306-6.

Mehtab, T., Yasin, G., Arif, M., Shakeel, M., Korai, R.M., Nadeem, M., Muhammad, N. and Lu, X. (2019), "Metal-organic frameworks for energy storage devices: Batteries and supercapacitors", *J. Energ. Storage*, **21**, 632-646. https://doi.org/10.1016/j.est.2018.12.025.

Milovancevic, M., Marinović, J.S., Nikolić, J., Kitić, A., Shariati, M., Trung, N.-T., Wakil, K. and Khorami, M. (2019), "UML diagrams for dynamical monitoring of rail vehicles", *Physica A*, 121169. https://doi.org/10.1016/j.physa.2019.121169.

Mohammadhassani, M., Nezamabadi-Pour, H., Suhatril, M. and Shariati, M. (2013), "Identification of a suitable ANN architecture in predicting strain in tie section of concrete deep beams", *Struct. Eng. Mech., Int. J.*, **46**(6), 853-868. http://doi.org/10.12989/sem.2013.46.6.853.

Mohammadhassani, M., Akib, S., Shariati, M., Suhatril, M. and Arabnejad Khanouki, M.M. (2014a), "An experimental study on the failure modes of high strength concrete beams with particular references to variation of the tensile reinforcement ratio", *Eng. Fail. Anal.*, **41**, 73-80. https://doi.org/10.1016/j.engfailanal.2013.08.014.

Mohammadhassani, M., Nezamabadi-Pour, H., Suhatril, M. and Shariati, M. (2014b), "An evolutionary fuzzy modelling approach and comparison of different methods for shear strength prediction of high-strength concrete beams without stirrups", *Smart Struct. Syst., Int. J.*, **14**(5), 785-809. http://doi.org/10.12989/sss.2014.14.5.785.

Mohammadhassani, M., Suhatril, M., Shariati, M. and Ghanbari, F. (2014c), "Ductility and strength assessment of HSC beams with varying of tensile reinforcement ratios", *Struct. Eng. Mech., Int. J.*, **48**(6), 833-848. https://doi.org/10.12989/sem.2013.48.6.833.

Naghipour, M., Niak, K.M., Shariati, M. and Toghroli, A. (2020a), "Effect of progressive shear punch of a foundation on a reinforced concrete building behavior", *Steel Compos. Struct., Int. J.*, **35**(2), 279-294. https://doi.org/10.12989/scs.2020.35.2.279.

Naghipour, M., Yousofizinsaz, G. and Shariati, M. (2020b), "Experimental study on axial compressive behavior of welded built-up CFT stub columns made by cold-formed sections with different welding lines", *Steel Compos. Struct., Int. J.*, **34**(3), 347. http://doi.org/10.12989/scs.2020.34.3.347.

Nasrollahi, S., Maleki, S., Shariati, M., Marto, A. and Khorami, M. (2018), "Investigation of pipe shear connectors using push out test", *Steel Compos. Struct., Int. J.*, **27**(5), 537-543. http://doi.org/10.12989/scs.2018.27.5.537.

Ngo, Q., Dang, D.N.M. and Tran, K.A. (2018), "Flying Height Optimization for Unmanned Aerial Vehicles in Cellular-Flying Adhoc Network", *J. Adv. Eng. Computat.*, **2**(4), 216-223. http://doi.org/10.25073/jaec.201824.210.

Ni, T., Chang, H., Song, T., Xu, Q., Huang, Z., Liang, H., Yan, A. and Wen, X. (2019a), "Non-intrusive Online Distributed Pulse Shrinking Based Interconnect Testing in 2.5 D IC", *IEEE T. Circuit II*, **67**(11), 2657-2661. https://doi.org/10.1109/TCSII.2019.2962824.

Ni, T., Yao, Y., Chang, H., Lu, L., Liang, H., Yan, A., Huang, Z. and Wen, X. (2019b), "LCHR-TSV: Novel low cost and highly repairable honeycomb-based TSV redundancy architecture for clustered faults", *IEEE T. Comput. Aid. D.*, **39**(10), 2938-2951. https://doi.org/10.1109/TCAD.2019.2946243.

Ning, X.H., Liao, C.Z. and Li, G.Q. (2020), "Electrochemical properties of Ca–Pb electrode for calcium-based liquid metal batteries", *Int. J. Miner. Metall. Mater.*, **27**(12), 1723-1729. https://doi.org/10.1007/s12613-020-2150-9.

Nosrati, A., Zandi, Y., Shariati, M., Khademi, K., Darvishnezhad Aliabad, M., Marto, A., Mu'azu, M., Ghanbari, E., Mandizadeh, M.B. and Shariati, A. (2018), "Portland cement structure and its major oxides and fineness", *Smart Struct. Syst., Int. J.*, **22**(4), 425-432. https://doi.org/10.12989/sss.2018.22.4.425.

Qi, C. and Fourie, A. (2019), "Cemented paste backfill for mineral tailings management: Review and future perspectives", *Mineral. Eng.*, **144**, 106025. https://doi.org/10.1016/j.mineng.2019.106025.

Qi, C., Chen, Q. and Kim, S.S. (2020), "Integrated and intelligent design framework for cemented paste backfill: A combination of robust machine learning modelling and multi-objective optimization", *Mineral. Eng.*, **155**, 106422. https://doi.org/10.1016/j.mineng.2020.106422.

Rajaei, S., Shoaei, P., Shariati, M., Ameri, F., Musaeei, H.R., Behforouz, B. and de Brito, J. (2021), "Rubberized alkali-activated slag mortar reinforced with polypropylene fibres for application in lightweight thermal insulating materials", *Constr. Build. Mater.*, **270**, 121430. https://doi.org/10.1016/j.conbuildmat.2020.121430.

Rouhanifar, S. and Afrazi, M. (2019), "Experimental study on mechanical behavior of sand-rubber mixtures", *Modares Civil Eng.*, **19**(4), 83-96. https://doi.org/10.4589/62457-246.6

Rouhanifar, S., Afrazi, M., Fakhimi, A. and Yazdani, M. (2020), "Strength and deformation behaviour of sand-rubber mixture", *Int. J. Geotech. Eng.*, 1-15. https://doi.org/10.1080/19386362.2020.1812193.

Safa, M., Shariati, M., Ibrahim, Z., Toghroli, A., Baharom, S.B., Nor, N.M. and Petkovic, D. (2016), "Potential of adaptive neuro fuzzy inference system for evaluating the factors affecting steel-concrete composite beam's shear strength", *Steel Compos. Struct., Int. J.*, **21**(3), 679-688. https://doi.org/10.12989/scs.2016.21.3.679.

Safa, M., Maleka, A., Arjomand, M.-A., Khorami, M. and Shariati, M. (2019), "Strain rate effects on soil-geosynthetic interaction in fine-grained soil", *Geomech. Eng., Int. J.*, **19**(6), 533. https://doi.org/10.12989/gae.2019.19.6.533.

Safa, M., Sari, P.A., Shariati, M., Suhatril, M., Trung, N.T., Wakil, K. and Khorami, M. (2020), "Development of neuro-fuzzy and neuro-bee predictive models for prediction of the safety factor of eco-protection slopes", *Physica A*, 124046. https://doi.org/10.1016/j.physa.2019.124046.

Sajedi, F. and Shariati, M. (2019), "Behavior study of NC and HSC RCCs confined by GRP casing and CFRP wrapping", *Steel Compos. Struct., Int. J.*, **30**(5), 417-432. https://doi.org/10.12989/scs.2019.30.5.417.

Sedghi, Y., Zandi, Y., Shariati, M., Ahmadi, E., Moghimi Azar, V., Toghroli, A., Safa, M., Tonnizam Mohamad, E., Khorami, M. and Wakil, K. (2018), "Application of ANFIS technique on performance of C and L shaped angle shear connectors", *Smart Struct. Syst., Int. J.*, **22**(3), 335-340. https://doi.org/10.12989/sss.2018.22.3.335.

Shah, S., Sulong, N.R., Shariati, M. and Jumaat, M. (2015), "Steel rack connections: Identification of most influential factors and a comparison of stiffness design methods", *PloS One*, **10**(10), e0139422. https://doi.org/10.1371/journal.pone.0139422.

Shah, S., Ramli Sulong, N.H., Shariati, M., Khan, R. and Jumaat, M. (2016a), "Behavior of steel pallet rack beam-to-column connections at elevated temperatures", *Thin Wall. Struct.*, **106**, 471-483. https://doi.org/10.1016/j.tws.2016.05.021.

Shah, S., Sulong, N.R., Khan, R., Jumaat, M. and Shariati, M. (2016b), "Behavior of industrial steel rack connections", *Mech. Syst. Signal Pr.*, **70**, 725-740. https://doi.org/10.1016/j.ymssp.2015.08.026.

Shahabi, S., Ramli Sulong, N.H., Shariati, M. and Shah, S. (2016), "Performance of shear connectors at elevated temperatures-A review", *Steel Compos. Struct., Int. J.*, **20**(1), 185-203. https://doi.org/10.12989/scs.2016.20.1.185.

Shariati, M. (2008). *Assessment of Building Using None-destructive Test Techniques (ultra Sonic Pulse Velocity and Schmidt Rebound Hammer)*, Universiti Putra Malaysia. https://doi.org/10.3245/DF123-234.4.

Shariati, M. (2013). *Behaviour of C-shaped Shear Connectors in Stell Concrete Composite Beams*, Jabatan Kejuruteraan Awam, Fakulti Kejuruteraan, Universiti Malaya. https://doi.org/10.1453/AS346-345.6.

Shariati, M. (2020), "Evaluation of seismic performance factors for tension-only braced frames", *Steel Compos. Struct., Int. J.*, **35**(4), 599-609. https://doi.org/10.12989/scs.2020.35.4.599.

Shariati, M., Ramli Sulong, N.H. and Arabnejad Khanouki, M.M. (2010), "Experimental and analytical study on channel shear connectors in light weight aggregate concrete", *Proceedings of the 4th international conference on Steel Compos. Struct.*, pp. 21-23. http://doi.org/10.3850/978-981-08-6218-3_CC-Fr031.

Shariati, M., Ramli Sulong, N.H., Arabnejad Khanouki, M.M. and Shariati, A. (2011), "Experimental and numerical investigations of channel shear connectors in high strength concrete", *Proceedings of the 2011 World Congress on Advances in Structural Engineering and Mechanics (ASEM'11+)*. https://doi.org/10.1448/812.3457.4587.

Shariati, M., Tahir, M.M., Wee, T.C., Shah, S., Jalali, A., Abdullahi, M.A.M. and Khorami, M. (2018), "Experimental investigations on monotonic and cyclic behavior of steel pallet rack connections", *Eng. Fail. Anal.*, **85**, 149-166. https://doi.org/10.1016/j.engfailanal.2017.08.014.

Shariati, M., Azar, S.M., Arjomand, M.-A., Tehrani, H.S., Daei, M. and Safa, M. (2019a), "Comparison of dynamic behavior of shallow foundations based on pile and geosynthetic materials in fine-grained clayey soils", *Geomech. Eng., Int. J.*, **19**(6), 473-484. https://doi.org/10.12989/gae.2019.19.6.473.

Shariati, M., Faegh, S.S., Mehrabi, P., Bahavarnia, S., Zandi, Y., Masoom, D.R., Toghroli, A., Trung, N.-T. and Salih, M.N. (2019b), "Numerical study on the structural performance of corrugated low yield point steel plate shear walls with circular openings", *Steel Compos. Struct., Int. J.*, **33**(4), 569-581. https://doi.org/10.1016/j.jcsr.2015.04.023.

Shariati, M., Heyrati, A., Zandi, Y., Laka, H., Toghroli, A., Kianmehr, P., Safa, M., Salih, M.N. and Poi-Ngian, S. (2019c), "Application of waste tire rubber aggregate in porous concrete", *Smart Struct. Syst., Int. J.*, **24**(4), 553-566. https://doi.org/10.12989/sss.2019.24.4.553.

Shariati, M., Mafipour, M.S., Mehrabi, P., Bahadori, A., Zandi, Y., Salih, M.N., Nguyen, H., Dou, J., Song, X. and Poi-Ngian, S. (2019d), "Application of a hybrid artificial neural network-particle swarm optimization (ANN-PSO) model in behavior prediction of channel shear connectors embedded in normal and high-strength concrete", *Appl. Sci.*, **9**(24), 5534. https://doi.org/10.3390/app9245534.

Shariati, M., Mafipour, M.S., Mehrabi, P., Zandi, Y., Dehghani, D., bahadori, A., Shariati, A., Trung, N.T., Salih, M.N. and Poi-Ngian, S. (2019e), "Application of Extreme Learning Machine (ELM) and Genetic Programming (GP) to design steel-concrete composite floor systems at elevated temperatures", *Steel Compos. Struct., Int. J.*, **33**(3), 319-332. https://doi.org/10.12989/scs.2019.33.3.319.

Shariati, M., Azar, S.M., Arjomand, M.-A., Tehrani, H.S., Daei, M. and Safa, M. (2020a), "Evaluating the impacts of using piles and geosynthetics in reducing the settlement of fine-grained soils under static load", *Geomech. Eng., Int. J.*, **20**(2), 87-101. https://doi.org/10.12989/gae.2020.20.2.087.

Shariati, M., Ghorbani, M., Naghipour, M., Alinejad, N. and Toghroli, A. (2020b), "The effect of RBS connection on energy absorption in tall buildings with braced tube frame system", *Steel Compos. Struct., Int. J.*, **34**(3), 393-407. https://doi.org/10.12989/scs.2020.34.3.393.

Shariati, M., Grayeli, M., Shariati, A. and Naghipour, M. (2020c), "Performance of composite frame consisting of steel beams and concrete filled tubes under fire loading", *Steel Compos. Struct., Int. J.*, **36**(5), 587-602. https://doi.org/10.12989/scs.2020.36.5.587.

Shariati, M., Mafipour, M.S., Mehrabi, P., Ahmadi, M., Wakil, K., Trung, N.T. and Toghroli, A. (2020d), "Prediction of concrete strength in presence of furnace slag and fly ash using Hybrid ANN-GA (Artificial Neural Network-Genetic Algorithm)", *Smart Struct. Syst., Int. J.*, **25**(2), 183-195. https://doi.org/10.12989/sss.2020.25.2.183.

Shariati, M., Naghipour, M., Yousofizinsaz, G., Toghroli, A. and Tabarestani, N.P. (2020e), "Numerical study on the axial compressive behavior of built-up CFT columns considering different welding lines", *Steel Compos. Struct., Int. J.*, **34**(3), 377-391. http://doi.org/10.12989/scs.2020.34.3.377.

Shariati, M., Shariati, A., Trung, N.T., Shoaei, P., Ameri, F., Bahrami, N. and Zamanabadi, S.N. (2020f), "Alkali-activated slag (AAS) paste: Correlation between durability and microstructural characteristics", *Constr. Build. Mater.*, 120886. https://doi.org/10.1016/j.conbuildmat.2020.120886.

Shariati, M., Tahmasbi, F., Mehrabi, P., Bahadori, A. and Toghroli, A. (2020g), "Monotonic behavior of C and L shaped angle shear connectors within steel-concrete composite beams: an experimental investigation", *Steel Compos. Struct., Int. J.*, **35**(2), 237-247. http:/.doi.org/10.12989/scs.2020.35.2.237.

Sharma, S., Kim, M.-S., Kim, D. and Yu, J.-S. (2013), "Al nanorod thin films as anode electrode for Li ion rechargeable batteries", *Electrochimica Acta*, **87**, 872-879. https://doi.org/10.1016/j.electacta.2012.09.028.

Shi, M., Wang, B., Shen, Y., Jiang, J., Zhu, W., Su, Y., Narayanasamy, M., Angaiah, S., Yan, C. and Peng, Q. (2020), "3D assembly of MXene-stabilized spinel ZnMn2O4 for highly durable aqueous zinc-ion batteries", *Chem. Eng. J.*, **399**, 125627. https://doi.org/10.1016/j.cej.2020.125627.

Si, Q., Hanai, K., Imanishi, N., Kubo, M., Hirano, A., Takeda, Y. and Yamamoto, O. (2009), "Highly reversible carbon–nano-silicon composite anodes for lithium rechargeable batteries", *J. Power Sources*, **189**(1), 761-765. https://doi.org/10.1016/j.jpowsour.2008.08.007.

Srither, S., Selvam, M., Arunmetha, S., Yuvakkumar, R., Saminathan, K. and Rajendran, V. (2013), "Enhancement of discharge capacity of Mg/MnO2 primary cell with Nano-MnO2 as cathode", *Sci. Adv. Mater.*, **5**(10), 1372-1376. https://doi.org/10.1166/sam.2013.1598.

Srither, S., Karthik, A., Selvam, M., Saminathan, K., Rajendran, V. and Kaler, K.V. (2014), "Nano-sized MnO_2 particles produced by spray pyrolysis for a Zn/MnO_2 primary cell: Comparative discharge performance studies with their bulk counterparts", *RSC Adv.*, **4**(79), 42129-42136. http://doi.org/10.1039/C4RA05060F.

Suhatril, M., Osman, N., Sari, P.A., Shariati, M. and Marto, A. (2019), "Significance of surface eco-protection techniques for cohesive soils slope in Selangor, Malaysia", *Geomech. Eng., Int. J.*, **37**(3), 2007-2014. https://doi.org/10.1007/s10706-018-0740-3.

Sun, Y., Wang, S., Dai, Y. and Lei, X. (2016), "Electrochemical characterization of nano V, Ti doped MnO_2 in primary lithium manganese dioxide batteries with high rate", *Funct. Mater. Lett.*, **9**(01), 1650005. https://doi.org/10.1142/S1793604716500053.

Tang, K., Mu, X., van Aken, P.A., Yu, Y. and Maier, J. (2013), "Nano-pearl-string" $TiNb_2O_7$ as anodes for rechargeable lithium

batteries", *Adv. Eng. Mater.*, **3**(1), 49-53. https://doi.org/10.1002/aenm.201200396.

Teki, R., Datta, M.K., Krishnan, R., Parker, T.C., Lu, T.M., Kumta, P.N. and Koratkar, N. (2009), "Nanostructured silicon anodes for lithium ion rechargeable batteries", *Small*, **5**(20), 2236-2242. https://doi.org/10.1002/smll.200900382.

Toghroli, A., Suhatril, M., Ibrahim, Z., Safa, M., Shariati, M. and Shamshirband, S. (2016), "Potential of soft computing approach for evaluating the factors affecting the capacity of steel–concrete composite beam", *J. Intell. Manuf.*, **29**(8). http://doi.org/10.1007/s10845-016-1217-y.

Toghroli, A., Shariati, M., Karim, M.R. and Ibrahim, Z. (2017), "Investigation on composite polymer and silica fume–rubber aggregate pervious concrete", *Proceedings of the Fifth International Conference on Advances in Civil, Structural and Mechanical Engineering - CSM 2017*, Zurich, Switzerland. http://doi.org/10.15224/978-1-63248-132-0-56.

Toghroli, A., Mehrabi, P., Shariati, M., Trung, N.T., Jahandari, S. and Rasekh, H. (2020), "Evaluating the use of recycled concrete aggregate and pozzolanic additives in fiber-reinforced pervious concrete with industrial and recycled fibers", *Constr. Build. Mater.*, **252**, 118997. https://doi.org/10.1016/j.conbuildmat.2020.118997.

Trung, N.T., Shahgoli, A.F., Zandi, Y., Shariati, M., Wakil, K., Safa, M. and Khorami, M. (2019a), "Moment-rotation prediction of precast beam-to-column connections using extreme learning machine", *Struct. Eng. Mech., Int. J.*, **70**(5), 639-647. https://doi.org/10.12989/sem.2019.70.5.639.

Trung, N.T., Alemi, N., Haido, J.H., Shariati, M., Baradaran, S. and Yousif, S.T. (2019b), "Reduction of cement consumption by producing smart green concretes with natural zeolites", *Smart Struct. Syst., Int. J.*, **24**(3), 415-425. https://doi.org/10.12989/sss.2019.24.3.415.

Wang, L., Huang, Y., Xie, Y. and Du, Y. (2020), "A new regularization method for dynamic load identification", *Sci. Prog.*, **103**(3), 0036850420931283. https://doi.org/10.1177%2F0036850420931283.

Wei, J.-H., Gao, X.-T., Tan, S.-P., Wang, F., Zhu, X.-D. and Yin, G.-P. (2017), "Acetylene black loaded on graphene as a cathode material for boosting the discharging performance of Li/SOCl2 battery", *Int. J. Electrochem. Sci.*, **12**, 898-905. http://doi.org/10.20964/2017.02.01.

Wei, X., Shariati, M., Zandi, Y., Pei, S., Jin, Z., Gharachurlu, S., Abdullahi, M.M., Tahir, M.M. and Khorami, M. (2018), "Distribution of shear force in perforated shear connectors", *Steel Compos. Struct., Int. J.*, **27**(3), 389-399 http://doi.org/10.12989/scs.2018.27.3.389.

Xie, Q., Sinaei, H., Shariati, M., Khorami, M., Mohamad, E.T. and Bui, D.T. (2019), "An experimental study on the effect of CFRP on behavior of reinforce concrete beam column connections", *Steel Compos. Struct., Int. J.*, **30**(5), 433-441 https://doi.org/10.12989/scs.2019.30.5.433.

Xing, Z., Ju, Z., Yang, J., Xu, H. and Qian, Y. (2012), "One-step hydrothermal synthesis of ZnFe 2 O 4 nano-octahedrons as a high capacity anode material for Li-ion batteries", *Nano Res.*, **5**(7), 477-485. https://doi.org/10.1007/s12274-012-0233-2.

Xu, Z., Li, H., Sun, H., Zhang, Q. and Li, K. (2010), "Carbon nanotubes with phthalocyanine-decorated surface produced by NH_3-assisted microwave reaction and their catalytic performance in Li/$SOCl_2$ battery", *Chinese J. Chem.*, **28**(10), 2059-2066. https://doi.org/10.1002/cjoc.201090344.

Yan, X., Huang, X., Chen, Y., Liu, Y., Xia, L., Zhang, T., Lin, H., Jia, D., Zhong, B. and Wen, G. (2021), "A theoretical strategy of pure carbon materials for lightweight and excellent absorption performance", *Carbon*, **174**, 662-672. https://doi.org/10.1016/j.carbon.2020.11.044.

Yang, C., Gao, F. and Dong, M. (2020a), "Energy efficiency modeling of integrated energy system in coastal areas", *J. Coastal Res.*, **103**(SI), 995-1001. https://doi.org/10.2112/SI103-207.1.

Yang, Y., Chen, H., Zou, X., Shi, X.-L., Liu, W.-D., Feng, L., Suo, G., Hou, X., Ye, X. and Zhang, L. (2020b), "Flexible carbon-fiber/semimetal Bi nanosheet arrays as separable and recyclable plasmonic photocatalysts and photoelectrocatalysts", *ACS Appl. Mater. Interf.*, **12**(22), 24845-24854. https://doi.org/10.1021/acsami.0c05695.

Yasin, G., Arif, M., Mehtab, T., Lu, X., Yu, D., Muhammad, N., Nazir, M.T. and Song, H. (2020), "Understanding and suppression strategies toward stable Li metal anode for safe lithium batteries", *Energy Storage Mater.*, **25**, 644-678. https://doi.org/10.1016/j.ensm.2019.09.020.

Yazdani, M., Kabirifar, K., Frimpong, B.E., Shariati, M., Mirmozaffari, M. and Boskabadi, A. (2020), "Improving construction and demolition waste collection service in an urban area using a simheuristic approach: A case study in Sydney, Australia", *J. Clean. Prod.*, **280**, 124138. https://doi.org/10.1016/j.jclepro.2020.124138.

Yoo, J.-K., Kim, J., Lee, H., Choi, J., Choi, M.-J., Sim, D.M., Jung, Y.S. and Kang, K. (2013), "Porous silicon nanowires for lithium rechargeable batteries", *Nanotechnology*, **24**(42), 424008. https://doi.org/10.1088/0957-4484/24/42/424008.

Yu, D., Mao, Y., Gu, B., Nojavan, S., Jermsittiparsert, K. and Nasseri, M. (2020), "A new LQG optimal control strategy applied on a hybrid wind turbine/solid oxide fuel cell/in the presence of the interval uncertainties", *Sustain. Energ. Grid. Network.*, **21**, 100296. https://doi.org/10.1016/j.segan.2019.100296.

Zhang, J., Chen, Q., Sun, J., Tian, L. and Zuo, C. (2020a), "On a universal solution to the transport-of-intensity equation", *Opt. Lett.*, **45**(13), 3649-3652. https://doi.org/10.1364/OL.391823.

Zhang, J., Sun, J., Chen, Q. and Zuo, C. (2020b), "Resolution analysis in a lens-free on-chip digital holographic microscope", *IEEE T. Comput.*, **6**, 697-710. https://doi.org/10.1109/TCI.2020.2964247.

Zhang, Y., Liu, G., Zhang, C., Chi, Q., Zhang, T., Feng, Y., Zhu, K., Zhang, Y., Chen, Q. and Cao, D. (2020c), "Low-cost MgFexMn2-xO4 cathode materials for high-performance aqueous rechargeable magnesium-ion batteries", *Chem. Eng. J.*, **392**, 123652. https://doi.org/10.1016/j.cej.2019.123652.

Zhang, J., Wang, M., Tang, Y., Ding, Q., Wang, C., Huang, X., Chen, D. and Yan, F. (2021), "Angular velocity measurement with improved scale factor based on a wideband-tunable optoelectronic oscillator", *IEEE T. Instrum. Meas.*, **70**, 1-9. https://doi.org/10.1109/TIM.2021.3067183.

Ziaei-Nia, A., Shariati, M. and Salehabadi, E. (2018), "Dynamic mix design optimization of high-performance concrete", *Steel Compos. Struct., Int. J.*, **29**(1), 67-75. https://doi.org/10.12989/scs.2018.29.1.067.

Zuo, C., Chen, Q., Tian, L., Waller, L. and Asundi, A. (2015), "Transport of intensity phase retrieval and computational imaging for partially coherent fields: The phase space perspective", *Opt. Laser. Eng.*, **71**, 20-32. https://doi.org/10.1016/j.optlaseng.2015.03.006.

Zuo, C., Sun, J., Li, J., Zhang, J., Asundi, A. and Chen, Q. (2017), "High-resolution transport-of-intensity quantitative phase microscopy with annular illumination", *Sci. Report.*, **7**(1), 1-22. https://doi.org/10.1038/s41598-017-06837-1.

Zuo, X., Dong, M., Gao, F. and Tian, S. (2020), "The modeling of the electric heating and cooling system of the integrated energy system in the coastal area", *J. Coastal Res.*, **103**(SI), 1022-1029. https://doi.org/10.2112/SI103-213.1.